

Study on Carbon Emission Reduction Countermeasures Based on Carbon Emission Influencing Factors and Trends

Tang Xinfu (✉ xinfatang@sina.com)

Jiangxi Science and Technology Normal University <https://orcid.org/0000-0002-8372-149X>

Liu Shuai

Jiangxi Science and Technology Normal University

Wang Yonghua

State Grid Jiangxi Electric Power Co Ltd

Wan Youwei

Jiangxi Science and Technology Normal University

Research Article

Keywords: Dual carbon target, STIRPAT model, PSO-BP neural network, Scenario analysis, Countermeasure

Posted Date: September 6th, 2023

DOI: <https://doi.org/10.21203/rs.3.rs-3242395/v1>

License:   This work is licensed under a Creative Commons Attribution 4.0 International License.

[Read Full License](#)

Version of Record: A version of this preprint was published at Environmental Science and Pollution Research on January 25th, 2024. See the published version at <https://doi.org/10.1007/s11356-024-31962-6>.

Study on Carbon Emission Reduction Countermeasures Based on Carbon Emission Influencing Factors and Trends

Tang Xinfan¹, Liu Shuai¹, Wang Yonghua², Wan Youwei¹

¹ School of Economic Management and Law, Jiangxi Science and Technology
Normal University, Nanchang 330013, Jiangxi, China

² State Grid Jiangxi Electric power CO.,LTD, China

*Corresponding author, email:xinfatang@sina.com

Abstract: In order to promote the achievement of the dual-carbon goal, this paper proposes an extended STIRPAT model and a PSO-BP neural network prediction model to analyze and predict the factors influencing carbon emissions and future carbon emissions. To address the multicollinearity problem, the STIRPAT model was validated using ridge regression, and the BP neural network was optimized using the particle swarm algorithm (PSO) to improve the prediction accuracy of the model. Taking the metal smelting industry in China as the research object, the results show that the influencing factors of carbon emission in the metal smelting industry are, in descending order, population size, energy structure, urbanization rate, intensity of energy consumption, added value of the secondary industry, and per capita GDP. In the future, the carbon emission of the metal smelting industry in China will keep the downward trend of the industry year by year, and the adjustment of the energy structure is the key to the achievement of carbon emission reduction in this industry. Finally, a series of countermeasures are proposed to reduce carbon emissions in the metal smelting industry with regard to the influencing factors and trends of carbon emissions.

Keywords: Dual carbon target, STIRPAT model, PSO-BP neural network, Scenario analysis, Countermeasure

1 Introduction

1.1 Literature Review

The development of human society has caused severe damage to the ecological environment. The Sixth Assessment Report of the Intergovernmental Panel on Climate Change (IPCC) states that global net anthropogenic GHG emissions in 2019 were 59 ± 6.6 (GtCO₂-eq), an increase of about 12% (6.5 GtCO₂-eq) and 54% (21 GtCO₂-eq) from 2010 and 1990, respectively, with fossil fuel combustion and industrial process emissions of CO₂ accounts for the largest share and increase in total GHG emissions. In 2019, about 79 % of global GHG emissions come from the energy, industry, transport, and building sectors, and CO₂ reductions are smaller than the increase in emissions from rising levels of global industry, energy supply, transport, agriculture, and building activities due to the increase in GDP energy intensity and energy carbon intensity. Countries around the world are facing a severe problem of carbon emissions. In recent years, many scholars have focused on the relationship between carbon dioxide and carbon emission influencing factors to carry out multifaceted research, which has important practical implications for adjusting and formulating carbon emission reduction policies. The effects of real GDP per capita, electricity consumption, trade openness, and demographic and financial development on pollutant emissions are investigated in Stochastic Effects of Population, Affluence, and Technology Regression (STIRPAT) in Southeast European (SEE) countries. A bidirectional causal relationship is found between electricity consumption and pollutant emissions and between trade openness and pollutant emissions. Also, unidirectional causality between real GDP per capita and pollutant emissions is revealed. These Southeastern European countries need to transition to renewable energy and energy-efficient technologies to sustain long-term economic growth (Verbič, M et al., 2022). The relationship between GDP per capita and carbon emissions per capita in China and the factors affecting carbon emissions in China are analyzed using the Environmental Kuznets Curve (EKC) and STIRPAT models. Economic growth is the most prominent factor influencing China's carbon emissions, followed by fossil fuel use (Zhang Qingyu et al., 2019). The Tapio

decoupling model was used to quantify the decoupling of CO₂ emissions from energy consumption and economic growth in China, and the overall decoupling between CO₂ emissions and economic growth was weak during 2000-2020 (Zhang J et al., 2023). This indicates that in the short term, China's economic growth and CO₂ emissions from energy consumption cannot be fully decoupled, and energy use efficiency needs to be improved. Specifically for the energy consumption in China's industrial sector, a decomposition model of energy consumption factors is constructed by combining the improved Kaya constant equation with the log-averaged Divisia index decomposition method (LMDI), and a decoupling effort index model is constructed on this basis. It is found that China's industrial economic growth and energy consumption are decoupled in recent years. However, the number of strongly decoupled industries and the value of the decoupling index is small. The energy intensity effect and economic output structure effect are the critical factors in achieving strong decoupling, while the energy structure effect hinders the decoupling (Ma Xiaojun et al., 2021). Therefore, reducing energy intensity, adjusting economic output structure, and optimizing energy structure are essential to save energy and reduce consumption in China's industrial sector. In addition, the urbanization rate also has a significant impact on carbon emissions. The STIRPAT model was applied to analyze the impact and difference of factors such as urbanization on carbon emissions in Jiangxi Province, a model of ecological civilization in China, and found that there is an inverted U-shaped non-linear relationship between economic factors and carbon emissions and that it is consistent with the EKC hypothesis. A 1% change in urbanization will lead to a 1.7377% increase in carbon emissions. A low population growth rate, high GDP per capita growth rate, and low energy intensity growth rate model are necessary to control future carbon emissions in Jiangxi Province (Lv, T et al., 2023). Meanwhile, there are also studies to explore the drivers of carbon emissions from the industry level. Studying the two-stage log-averaged Dithering Decomposition (LMDI) and STIRPAT models for the steel industry, it was concluded

that the scale effect is the main factor promoting carbon emissions in the steel industry and energy intensity is the most significant inhibiting factor (Pan Chongchao et al., 2023) and that reducing fossil energy consumption and replacing fossil energy with non-fossil energy in the steel industry is the key for the industry. Similarly, the LMDI-STIRPAT model was applied to the study of carbon emissions from the plantation industry. It was found that the production efficiency of the plantation industry was the most critical factor in inhibiting carbon emissions. The country's economic development level was the most important influencing factor for the growth of carbon emissions (Cai Jingli et al., 2023). There is some variability in the influencing factors of carbon emissions in different industries. However, the level of national economic development is an important influencing factor of carbon emissions in each industry. Furthermore, from a regional perspective, carbon emission influencing factors in four major regions of China, namely, East, Northeast, West, and Central, play a differential role in the contribution of carbon emissions in different regions (Liu Yk et al., 2019). At the same time, 30 provinces in China were divided into three regions according to the electrification rate criterion to examine the relationship between energy intensity, energy consumption structure, population density, urbanization rate, and carbon intensity. Short-term effects and long-term relationships were found to exist across regions, with different influencing factors in different regions. However, in general, energy consumption structure and population density had a greater impact on carbon intensity (Sun, J et al., 2022). When specific to provinces and cities, population and population-related urbanization rates become the dominant factors of carbon emissions, followed by GDP level (Zhang Zhe et al., 2020; Zhao C et al., 2022). Fully exploring the various factors that influence carbon emissions is of great practical importance for different regions and countries to achieve carbon reduction. Structural changes in the economy are important influencing factors that contribute to the socioeconomic growth and ecological quality of countries. Turkey's dependence on fossil fuel energy

consumption has led to an unsustainable trajectory of economic development. Therefore, the best option for the local government is to encourage investment in the service sector to maintain an appropriate level of environmental sustainability (Adebayo, T.S et al., 2023). In Pakistan, economic expansion, growth, development, and agricultural production have led to a decline in local carbon emissions, which in turn has improved environmental conditions. In response, government and industry policymakers have encouraged people to use renewable energy and encourage them to invest more in green-related businesses (Ali, H.S et al., 2023). Reducing carbon emissions has become an important climate issue worldwide. Recently, the relationship between carbon dioxide emissions and information and communication technology (ICT) and financial development has also been revealed. The promotion of ICT has become one of the key technologies to reduce CO₂ emissions in the GCC countries (Islam, M.S et al., 2023).

It is not enough to analyze the factors influencing carbon emissions, but it is also necessary to forecast future carbon emissions. The current forecasting for carbon emissions mainly includes simulation and scenario analysis methods and the establishment of forecasting models. For instance, by building a system dynamics model of transportation carbon emissions, the effects of implementing different transportation emission reduction strategies were simulated (Xiao H et al., 2023). The integrated SD-VS model was built using the advantages of dynamic simulation of system dynamics (SD) and intelligent analysis of VisualStudio (VS) to predict the carbon emission trend and carbon peak time in Sichuan Province from 2020 to 2050 (Qiaochu Li et al., 2021). However, most scholars used the STIRPAT extended model and scenario analysis method to predict carbon emissions. It is found that there are significant differences in carbon emissions among the three provinces and one city in the Yangtze River Delta of China, and the carbon emission differences as a whole fluctuate and increase over time. The carbon emissions of the three provinces and one

city will reach the carbon peak by 2030 (Zou Xiuqing et al., 2023) Using the STIRPAT model, four carbon peaking action scenarios of the benchmark development, industry optimization, technology breakthrough, and low carbon development were established to predict the carbon peaking of the thermal power industry in Zhejiang Province from 2021 to 2035 (Zhang, C et al., 2023) The study results provide a theoretical basis and benchmark for promoting industrial restructuring and low-carbon transformation in China's thermal power industry through comprehensive management. The effects of population, GDP per capita, urbanization rate, industrial structure, energy consumption, energy mix, regional electrification rate, and openness to the outside world on carbon emissions are analyzed, and the influencing factors are incorporated into the STIRPAT model for modeling analysis. It was found that the carbon emissions of Shanghai's electric energy could peak by 2030 under the four development scenarios set (Wang H et al., 2022) An extended STIRPAT model was constructed by calculating the carbon dioxide emissions of transportation in Shanghai from 2003 to 2019 and making projections. It is found that oil consumption is the main source of carbon emissions from transportation and that under various scenarios (baseline scenario, technological stability-high growth, technological stability-low growth, technological progress-high growth, technological progress-low growth), the Shanghai transportation sector can reach peak CO₂ emissions by 2030 (Liping Zhu et al., 2022). Meanwhile, many scholars have applied machine learning methods to predict carbon emissions. For example, BP neural network models for predicting CO₂ emissions from buildings were developed by introducing influencing factors such as population, GDP, and gross construction output as model parameters (Pu X et al., 2022), combining artificial neural network (ANN) parameterization methods and vector autoregression (VAR) estimation to predict economic growth and net trade effects based on different types of renewable energy consumption (Mutascu, M et al., 2022), A combined gray model, cubic exponential smoothing, and gray cubic exponential smoothing model was used to

forecast transportation CO₂ emissions and make policy recommendations for CO₂ emission reduction paths in China's transportation industry (Li, Y et al., 2021), a KLS algorithm that integrates Kalman filter (KF), long and short-term memory (LSTM), and support vector machine (SVM) was proposed to achieve the integration of time series forecasting and variable regression (Yan Li et al., 2020), using various methods such as neural network time series nonlinear autoregression, Gaussian process regression, and Holt's method to forecast CO₂ emissions in Bahrain (Qader, M.R et al., 2022), using carbon emission forecasting as a research object, we established a method that integrates the least absolute shrinkage selection operator (LASSO), principal component analysis (PCA), support vector regression (SVR), and Differential Evolution-Grey Wolf Optimization (DE-GWO) in one integrated model (Shi, M et al., 2022), applied the classical Fibonacci series optimization theory and golden partition theory to the gray prediction model of approximate non-simultaneous exponential series and established a new optimization model (Tong, M et al., 2021), used Markov transfer matrix to predict the energy mix share of Fujian Province in the next 4 years, and predicted the carbon intensity target in 2025 can be achieved under the ordinary and energy-saving models, while the carbon intensity target cannot be achieved under the energy-consumption model (Lin X et al., 2022) A hybrid model combining the marine predator algorithm (MPA) and multicore support vector regression predicts that China's carbon dioxide emissions will continue to show a slow growth rate during the 14th Five-Year Plan period (Qin, X et al., 2023), an improved gray multivariate convolutional integration model (AGMC(1,N)) (Wang, M et al., 2022), a grey model of carbon emission dynamics was developed using neural networks by combining the modeling mechanism of classical feedforward neural network models with the role of external influences on carbon emissions (Nie, W et al., 2023), a genetic algorithm extreme value learning machine (GA-ELM) algorithm was used to predict carbon emissions in the Beijing-Tianjin-Hebei (BTH) region. The prediction of carbon

emissions in the Beijing-Tianjin-Hebei (BTH) region was carried out using the Genetic Algorithm Extreme Value Learning Machine (GA-ELM) algorithm, which showed that the improvement of energy intensity and energy consumption structure had the greatest contribution to carbon emission reduction. It verified the significant role of coordinated development strategies in promoting regional carbon emission reduction (Huang, Y et al.,2023). In order to evaluate the accuracy of different prediction models, a comparative analysis of different models has been carried out. BP neural network, LSTM network, and PSO-LSTM model were used to predict the peak carbon emission of buildings based on the comparison and selection of carbon emission prediction (Tang X.L et al., 2023), three neural network algorithms, BP, GA-BP, and PSO-BP, were used to construct the short-term prediction model of photovoltaic power generation. It was verified that the particle swarm algorithm has better applicability (Li Yuanqi et al., 2022).

1.2 Problem Statement

Throughout the literature at home and abroad, most scholars have focused on the power industry, transportation sector, construction industry, and various regions, but studies on carbon emissions in the metal smelting industry are rare. As a key industry with high energy consumption and carbon emissions, the metal smelting industry has a great impact on the climate and environment. A study on the factors influencing carbon emissions and carbon emission prediction in the metal smelting industry can provide a good guide for the implementation of national carbon emission reduction policies and also provide important theoretical support for the promotion of ecological civilization. The main contribution of this paper is to propose the STIRPAT model for carbon emissions in the metal smelting industry, which is used to analyze the potential relationship between various influencing factors and carbon emissions. At the same time, the influencing factors in the STIRPAT model are used as inputs to a BP neural network to forecast future carbon emission trends. Considering the lack of prediction

accuracy of the original BP neural network, the particle swarm (PSO) algorithm is introduced in this paper to optimize the BP neural network. In addition, most studies have used the STIRPAT model for scenario prediction or applied various prediction models for carbon emission prediction. In this paper, the STIRPAT model is applied for the first time to study the factors influencing carbon emissions in the metal smelting industry, and the optimized PSO-BP model is used to forecast carbon emissions for this industry. While verifying the applicability of the model, it provides policy recommendations for carbon emission reduction in the metal smelting industry and also provides some reference value for related studies in other industries.

2 Research Methods And Models

2.1 Carbon Accounting Methodology

Since China does not officially publish CO₂ emission data, other relevant data are needed to estimate carbon emissions. In this paper, the estimation of carbon emission data from metal smelting in China is based on the formula in the emission guidelines issued by IPCC (United Nations Intergovernmental Panel on Climate Change), and the estimation formula is as follows:

$$I = \sum Si \times Ei \quad (1)$$

In equation (1): I denotes carbon emission, Si denotes energy consumption, Ei denotes carbon emission coefficient of energy, i denotes energy type, representing coal, coke, crude oil, gasoline, kerosene, diesel, fuel oil, natural gas, and since electricity does not produce carbon emission in the process of use, the carbon emission impact of electricity is not considered in this paper. The specific energy carbon emission coefficients are shown in Table 1.

Table 1: Carbon emission coefficient of all kinds of energy

type of energy	coal	coke	crude	gasoline	kerosene	diesel	fuel oil	natural
source			oil			oil		gas

carbon emission								
factor(kgce/kg)	0.756	0.855	0.59	0.59	0.57	0.59	0.62	0.448

2.2 STIRPAT Model

STIRPAT is a scalable stochastic environmental impact assessment model that evaluates the relationship between human factors and the environment. The model equation is:

$$I=a \times P^b \times A^c \times T^d \times e \quad (2)$$

In equation (2): I , P , A , and T are environmental indicators, population, affluence, and technology, respectively, where affluence is expressed by GDP per capita and technology is expressed by energy consumption intensity, a is the model coefficient, b , c , and d are the indices of the respective variables, and e is the random error term.

To reduce the effect of heterogeneity among independent variables and to facilitate subsequent analysis, the STIRPAT model is taken as the natural logarithm and equation (2) is deformed as:

$$\ln I = \ln a + b \ln P + c \ln A + d \ln T + \ln e \quad (3)$$

The level of urbanization in China has been increasing with rapid economic development, but it has also caused serious environmental pollution. The actual energy consumption structure and intensity represent the technical level of the industry to a certain extent, metal smelting belongs to the secondary industry, and the output value of the whole industry should also be analyzed as a carbon emission factor. Therefore, this paper introduces urbanization rate (U) when measuring affluence, energy structure (C), energy consumption intensity (S), and value-added of secondary industry (D) when measuring technology level, where energy structure is expressed as the ratio of coal to total energy consumption and energy consumption intensity is expressed as the ratio of total energy consumption to GDP. The STIRPAT model was extended as follows:

$$\ln I = \ln a + \beta_1 \ln P + \beta_2 \ln A + \beta_3 \ln U + \beta_4 \ln C + \beta_5 \ln S + \beta_6 \ln D + \ln e \quad (4)$$

$\beta_1, \beta_2, \beta_3, \beta_4, \beta_5$, and β_6 are the regression coefficients of each influencing factor, respectively.

2.3 PSO-BP Neural Network Model

2.3.1 BP Neural Network

BP neural network is an artificial neural network that simulates the human brain to process problems and mimics the structural features of the human brain's nervous system to deal with complex problems in a distributed and parallel manner. BP neural network has input layer nodes, output layer nodes, and a hidden layer. The implementation of the BP neural network is divided into two steps. The first part is forward input propagation, where the input signal is processed by the input layer nodes and passed to the implicit layer nodes. In the implicit layer, the neurons of each unit act as activation functions to process the information. The processed information is transmitted to the output layer nodes to obtain the output results. The second part is backpropagation. The error signal returns along the original connection path when the output layer's output does not reach the expected output value. Meanwhile, the weights and thresholds of neurons in each layer are iteratively corrected to minimize the error signal. The learning process of the BP neural network ends when the error meets the set requirements. Figure 1 shows the structure of the BP neural network.

The basic computational steps of the BP neural network are as follows.

(1) Initialization of the network. In this study, the number of nodes in the input layer is 6, the number of nodes in the hidden layer is determined to be 4 by calculation and verification, and the number of nodes in the output layer is 1. The weight of the input layer to the hidden layer is w_{ij} , the weight of the hidden layer is w_{jk} , the threshold of the input layer to the hidden layer is b_j , and the threshold of the hidden layer to the output layer is b_k . The learning rate is η , and the activation function is $S(x)$. The activation function of this study is chosen as the Sigmoid function, which has the

characteristic that the derivative function is its own expression. As shown in equations (5) and (6):

$$S(x) = \frac{1}{1+e^{-x}} \quad (5)$$

$$S'(x) = \frac{e^{-x}}{(1+e^{-x})^2} = S(x)(1 - S(x)) \quad (6)$$

(2) Calculation of the output value H_j of the hidden layer.

$$H_j = S(\sum_{i=1}^6 w_{ij}x_i + b_j) \quad (7)$$

(3) Calculation of the output value O_k for the output layer.

$$O_k = \sum_{j=1}^4 H_j w_{jk} + b_k \quad (8)$$

(4) Calculate the error E between the output value O_k and the desired output value EO_k .

$$E = \frac{1}{2} (EO_k - O_k)^2 \quad (9)$$

(5) The error between the output value and the desired output value is back-propagated through the original path, and the gradient descent method is used to correct the weights and thresholds.

$$\frac{\partial E}{\partial w_{jk}} = (EO_k - O_k) \left(-\frac{\partial O_k}{\partial w_{jk}} \right) = (EO_k - O_k) (-H_j) \quad (10)$$

$$\frac{\partial E}{\partial w_{ij}} = \frac{\partial E}{\partial H_j} \cdot \frac{\partial H_j}{\partial w_{ij}} \quad (11)$$

$$\frac{\partial E}{\partial H_j} = (EO_k - O_k) \left(-\frac{\partial O_k}{\partial H_j} \right) = -w_{jk} (EO_k - O_k) \quad (12)$$

$$\frac{\partial H_j}{\partial w_{ij}} = \frac{\partial S(\sum_{i=1}^6 w_{ij}x_i + b_j)}{\partial w_{ij}} = H_j(1 - H_j)x_i \quad (13)$$

$$w_{jk}^+ = w_{jk} - \eta \frac{\partial E}{\partial w_{jk}} = w_{jk} + \eta H_j (EO_k - O_k) \quad (14)$$

$$w_{ij}^+ = w_{ij} - \eta \frac{\partial E}{\partial w_{ij}} = w_{ij} + \eta H_j x_i w_{jk} (1 - H_j) (EO_k - O_k) \quad (15)$$

$$\frac{\partial E}{\partial b_k} = (EO_k - O_k) \left(-\frac{\partial O_k}{\partial b_k} \right) = -(EO_k - O_k) \quad (16)$$

$$\frac{\partial E}{\partial b_j} = \frac{\partial E}{\partial H_j} \cdot \frac{\partial H_j}{\partial b_j} \quad (17)$$

$$\frac{\partial E}{\partial H_j} = (EO_k - O_k) \left(-\frac{\partial O_k}{\partial H_j} \right) = -w_{ij} (EO_k - O_k) \quad (18)$$

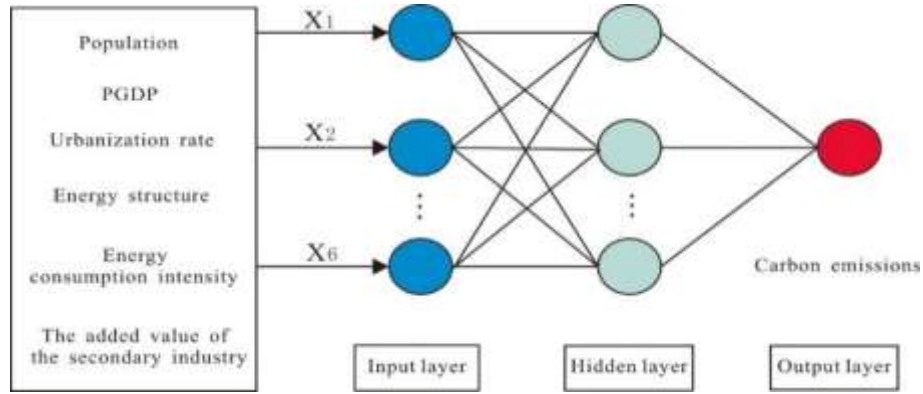
$$\frac{\partial H_j}{\partial b_j} = \frac{\partial S(\sum_{i=1}^6 w_{ij} x_i + b_j)}{\partial b_j} = H_j (1 - H_j) \quad (19)$$

$$b_k^+ = b_k - \eta \frac{\partial E}{\partial b_k} = b_k + \eta (EO_k - O_k) \quad (20)$$

$$b_j^+ = b_j - \eta \frac{\partial E}{\partial b_j} = b_j + \eta H_j w_{ij} (1 - H_j) (EO_k - O_k) \quad (21)$$

(6) The iteration is not considered complete until the maximum number of iterations or the target error is reached.

Figure 1: BP neural network structure diagram



2.3.2 PSO Algorithm

PSO is a group intelligence optimization algorithm derived from birds' feeding behavior in nature. During bird foraging, each bird usually follows the one closest to the food and looks around for food. Similar to genetic algorithms (Li Yuanqi et al.), particle swarm algorithms use the fitness of individuals in a population to evaluate the cost of individuals but do not perform crossover and mutation operations. In a population containing information about each weight and threshold in the BP neural network, each particle is characterized by three metrics: particle position, velocity, and fitness. The optimal initialized weights and thresholds of the BP neural network are obtained by tracking the optimal positions of individuals and populations. Thus, the BP neural network's convergence speed and prediction performance are improved.

The algorithm is constructed as follows:

1) Initialization of parameters.

2) Calculate the value of the fitness function and optimization functions' values as follows.

$$f_i = \sum_{x=1}^K (y_{ix} - Y_{ix})^2 \quad (22)$$

$$fit_s = \frac{1}{N} \sum_{i=1}^N f_i \quad (23)$$

where K is the output node, y_{ix} is the true output value of the i th particle at the x th node, and Y_{ix} is the desired output value. N is the overall size.

3) Update the individual optimal value and the global optimal value.

Suppose there are m particles in the population in the multidimensional search space, and the position and velocity of the i th particle in the t th iteration are $X_{i,t}$ and $V_{i,t}$, respectively. The particle updates itself by supervising two extremes: the first one is the best solution found by the particle itself, called the individual extremum (denoted by pb), and the other one is the optimal solution found by the current population, called the global extremum (denoted by gb).

4) The velocity and position are updated, and the updated position and velocity are given in the following equation:

$$V_{i,t+1} = w \times V_{i,t} + c_1 r_1 \times (pb_i - x_{i,t}) + c_2 r_2 \times (gb_i - x_{i,t}) \quad (24)$$

$$X_{i,t+1} = X_{i,t} + \lambda V_{i,t+1} \quad (25)$$

Where t is the number of iterations. w is the inertia weight, usually between 0.1 and 0.9, c_1 and c_2 are the learning factors, which regulate the maximum step of flight in the direction of the global best particle and the individual best particle, usually set $c_1 = c_2 = 2$. r_1 and r_2 are random numbers between [0,1]. λ is the velocity coefficient, usually taken as 1.

5) Algorithm termination. Conditions for terminating the algorithm: The number of iterations reaches the maximum, or the error reaches the target error.

2.3.3 PSO Algorithm to Optimize BP neural networks

The BP neural network algorithm can fit various complex nonlinear relationships between arbitrary inputs and outputs through continuous training and learning and has certain robustness and generalization ability. However, BP neural network algorithm has inherent shortcomings. BP neural network algorithm uses the standard gradient descent algorithm, which is easy to fall into local extremes during data training, resulting in data training failure. At the same time, the BP algorithm has the disadvantage of the data overfitting phenomenon. Generally speaking, the prediction ability of a neural network is proportional to the sample training ability. As the sample training ability increases, the prediction ability of the BP neural network reaches a limit and then decreases, which is the so-called overfitting phenomenon. To address the above shortcomings of the BP neural network algorithm, this paper adopts a particle swarm algorithm to optimize the structure of the BP neural network.

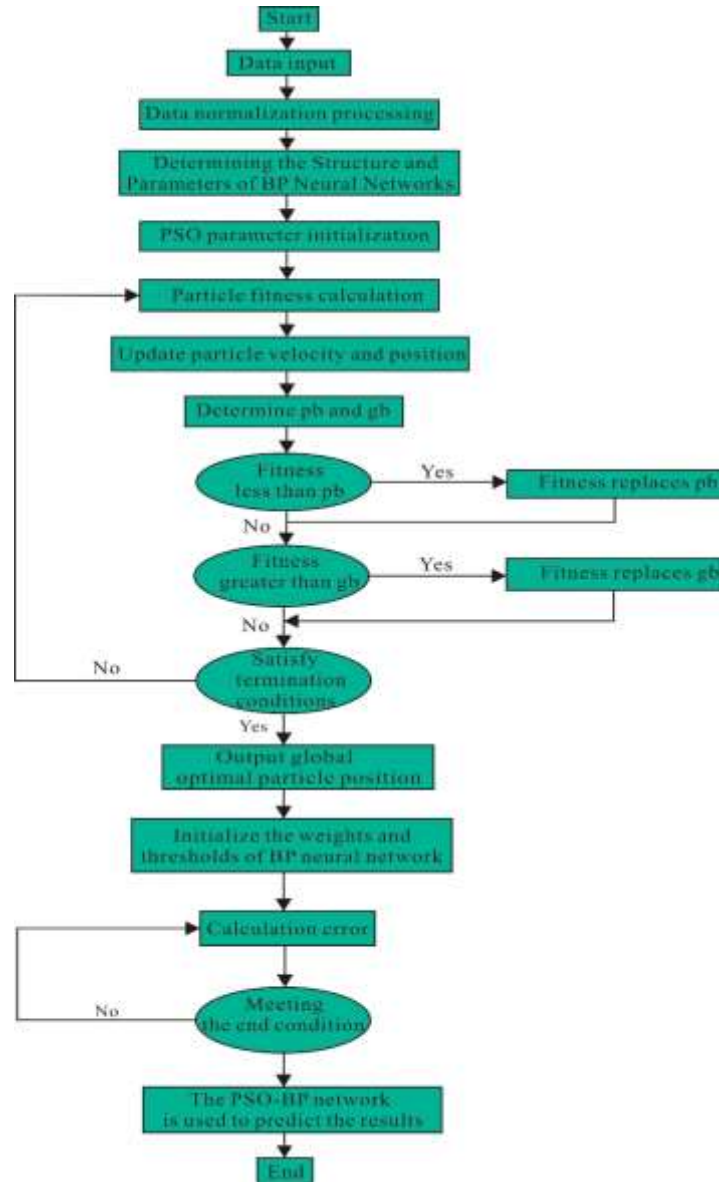
The initial number of nodes of the hidden layer neuron S is determined by the empirical equation (26).

$$S = \sqrt{m + n} + a \quad (26)$$

Where m is the number of neurons in the input layer, n is the number of neurons in the output layer, S is the number of neurons in the hidden layer, and a is an integer from 1 to 10.

In the BP neural network constructed in this paper, each sample has six inputs and one output. Then, the number of nodes in the hidden layer is gradually adjusted by the trial-and-error method. The neural network error is minimized by calculating the mean square error of the training data corresponding to a from 1 to 10. Finally, the number of nodes in the hidden layer is set to 4.

Figure 1: PSO optimized BP neural network structure diagram



382 A size $6 \times 4 \times 1$ network is set up, and a feedforward function is used to build a BP
 383 neural network. The network returns the error signal along the original path and updates
 384 the weights accordingly. The network achieves the desired output by iteratively
 385 modifying the weights and thresholds. The optimal weights are obtained by recursively
 386 updating the network weights in the case of error minimization. To find the appropriate
 387 model size and solve the overfitting problem of the BP neural network, first set smaller
 388 parameters for training and then start adjusting the parameter size until the minimum
 389 error is reached on the validation set. Through several iterations of testing, the

connection weights of each network layer were determined. The data were trained for several learning sessions to determine each model parameter of the BP neural network, where the learning rate was 0.001, the maximum number of cycle iterations was 1000, and the minimum error of the network was 0.00001.

The parameters of the PSO algorithm are acceleration factors c_1 and c_2 , population size n , position boundaries $[P_{min}, P_{max}]$, minimum and maximum velocities $[V_{min}, V_{max}]$, number of iterations T and inertia weight w . These parameters are set as shown in Table 2:

Table 2: PSO algorithm parameters table

parameter	c_1	c_2	n	w	T	P_{min}	P_{max}	V_{min}	V_{max}
value	2	2	4	0.9	30	-1	1	-1	1

2.4 Ridge regression analysis

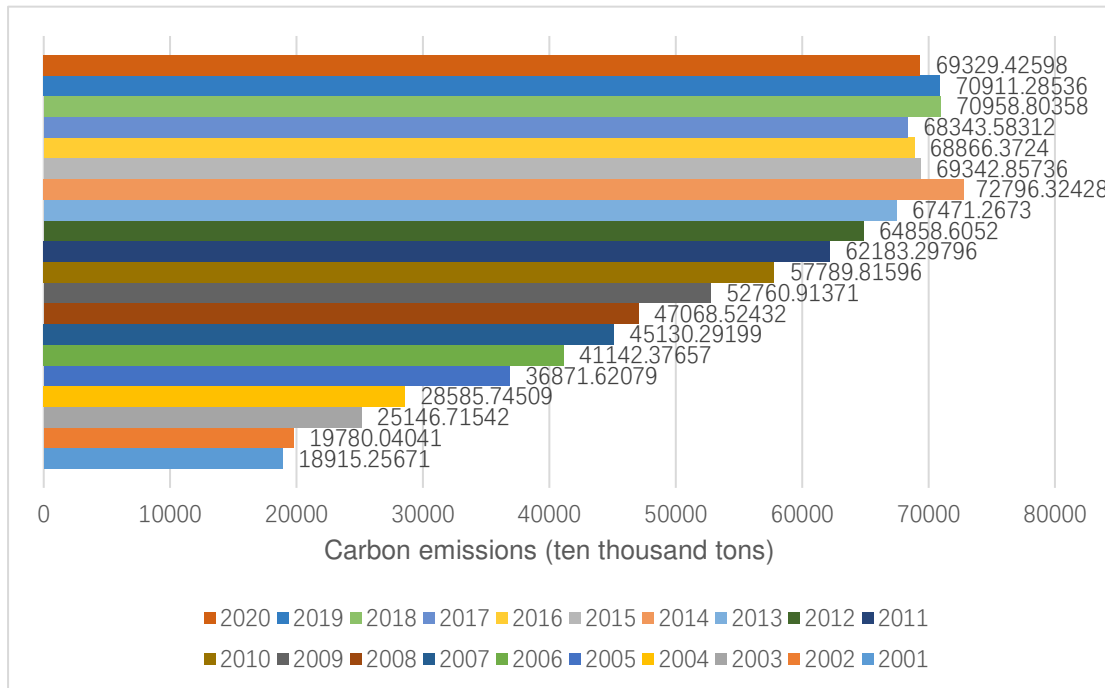
Ridge regression analysis is obtained by improving the least squares method with unbiased nature, which obtains regression coefficients at the cost of losing some information and reducing accuracy. It is a more realistic and reliable regression method, and the fit to the pathological data is stronger than the least squares method. It helps to alleviate the problems of multicollinearity and overfitting. In this paper, SPSS software was used to perform a ridge regression analysis of each influencing factor of the STIRPAT model.

3 Model Construction And Data Analysis

3.1 Data Sources and Description

The data on population size, GDP, and urbanization rate are from China Statistical Yearbook (2022), the urbanization rate is expressed as the ratio of the urban resident population to the total population, and the data on energy consumption and value-added secondary industry are from the National Bureau of Statistics.

Figure 2: China's Metal Smelting 2000-2020 Carbon Emissions



3.2 Analysis of the current situation of carbon emissions

The annual carbon emissions from metal smelting in China showed an overall fluctuating upward trend (see Figure 2). However, there was a brief decline from 2014 to 2017, probably due to the implementation of the Action Plan for Low Carbon Development of Energy Conservation and Emission Reduction in 2014-2015, which made the metal smelting industry pay more attention to carbon emission issues and thus brought about a short-term decline in carbon emissions. Carbon emissions started to rise slowly again after 2017. In order to explore its influence mechanism, further in-depth analysis of its influence factors is conducted.

3.3 Multicollinearity analysis

The variance inflation factor (VIF) is an indicator used to measure the relationship of multiple covariances between the selected variables and other variables. The formula is:

$$VIF_i = \frac{1}{1-R_i^2} \quad (27)$$

Where VIF_i represents the variance inflation factor of the i th selected variable. R_i^2 represents the correlation coefficient between the i th variable and other variables.

When the variance inflation factor exceeds 10, this paper considers that the variable has the problem of multicollinearity, and the larger the variance inflation factor is, the more serious the multicollinearity is. This paper uses SPSS software to conduct multiple linear regression analysis, and the VIF values of InP, InA, InU, InS, and InD are all greater than 10, indicating that there is multicollinearity among the independent variables.

Table 3: Carbon emission data of metal smelting in China and its influencing factors

year	Population (tens of millions)	PGDP (yuan / person)	Urbanization rate (%)	Energy structure (%)	Energy	The added	Carbon
					consumption intensity (tons / one hundred thousand yuan)	value of the secondary industry (billions)	emissions (ten thousand tons)
2001	1276.27	8717	37.66	59.04	0.22	49069	18915.26
2002	1284.53	9506	39.09	58.09	0.21	52982	19780.04
2003	1292.27	10666	40.53	56.68	0.23	61778	25146.72
2004	1299.88	12487	41.76	55.19	0.22	72387	28585.75
2005	1307.56	14368	42.99	51.67	0.25	86208	36817.62
2006	1314.48	16738	44.34	52.37	0.23	102004	41142.38
2007	1321.29	20494	45.89	52.07	0.21	121381	45130.29
2008	1328.02	24100	46.99	52.34	0.18	146183	47068.52
2009	1334.50	26180	48.34	50.90	0.19	156958	52760.91
2010	1340.91	30808	49.95	52.29	0.17	186481	57789.82
2011	1349.16	36277	51.83	53.05	0.16	220592	62183.30
2012	1359.22	39771	53.10	51.35	0.15	235319	64858.61
2013	1367.26	43497	54.49	52.21	0.14	249684	67471.27

2014	1376.46	46912	55.75	54.90	0.14	271392	72796.32
2015	1383.26	49922	57.33	56.04	0.13	274278	69342.86
2016	1392.32	53783	58.84	54.43	0.12	296236	68866.37
2017	1400.11	59592	60.24	55.21	0.10	334623	68343.58
2018	1405.41	65534	61.50	57.50	0.10	366001	70958.80
2019	1410.08	70078	62.71	54.96	0.09	386165	70911.29
2020	1412.12	71828	63.89	52.46	0.09	384255	69329.43

437

438

Table 4: Multicollinearity analysis

Model	Standardized					Collinearity statistics	
	Non-normalized coefficients		coefficient				
	Standard						
	B	Error	Beta	t	significance	allowance	VIF
constant	-30.097	22.441		-0.343	0.202		
lnP	4.845	3.566	0.358	1.358	0.197	0.001	799.883
lnA	0.275	0.316	-0.435	0.871	0.400	0.000	2867.368
lnU	-0.994	0.987	-0.372	-1.007	0.332	0.001	1568.722
lnC	-0.082	0.176	-0.008	-0.469	0.647	0.285	3.505
lnS	0.899	0.066	0.677	13.653	<0.001	0.035	28.283
lnD	0.752	0.249	1.163	3.015	0.010	0.001	1712.017

Table 5: Collinearity diagnostics

dimension	eigenvalue	condition index	variance ratio						
			(constant)	lnP	lnA	lnU	lnC	lnS	lnD
1	6.936	1	0	0	0	0	0	0	0
2	0.023	17.488	0	0	0	0	0	0.03	0

3	0.001	84.812	0	0	0	0	0.01	0.15	0
4	2.387×10^{-5}	540.598	0	0	0	0	0.72	0.31	0
5	9.016×10^{-6}	879.652	0	0	0	0.09	0.01	0.33	0.04
6	7.770×10^{-7}	2996.325	0	0	0.99	0.09	0.08	0.17	0.95
7	1.389×10^{-8}	22413.017	1	1	0	0.83	0.18	0	0.01

3.4 Ridge regression analysis

The results of the ridge regression show that based on the F-test significance p-value of 0.001, the level presents significance and rejects the original hypothesis, indicating a regression relationship between the independent and dependent variables. At the same time, the goodness of fit of the model R^2 is 0.987, and the model performs more and more excellently.

The equation of the obtained model is:

$$\ln I = -6.548 + 2.078 \times \ln P + 0.251 \times \ln A + 0.564 \times \ln U - 1.339 \times \ln C + 0.485 \times \ln S + 0.318 \times \ln D \quad (28)$$

$$I = 0.0014 \times P^{2.078} \times A^{0.251} \times U^{0.564} \times C^{-1.339} \times S^{0.485} \times D^{0.318} \quad (29)$$

According to equation (29), it can be concluded that: population size, GDP per capita, urban change rate, energy consumption intensity, and value-added of the secondary industry have a facilitating effect on the increase of carbon emissions from metal smelting in China, and each 1% increase of the above factors will increase carbon emissions by 2.078%, 0.251%, 0.564%, 0.485%, and 0.318%, respectively. Energy structure suppresses the increase of carbon emissions, and each 1% increase will cause a -1.339% change in carbon emissions. The energy structure has a suppressive effect on the increase of carbon emissions; each 1% increase will cause a change of -1.339%. Population size has the most significant impact on carbon emissions, indicating that an increase in population causes an increase in the average demand for metals, indirectly leading to an increase in energy consumption and carbon emissions. At the same time, GDP per capita and value-added of secondary industries positively contribute to carbon

emissions, indicating that decoupling carbon emissions from the economy cannot be achieved in the short term. The urbanization rate and energy consumption intensity, as necessary measures of development, also have different degrees of impact on carbon emissions, and there are still urgent problems to be solved for carbon emission reduction in the metal smelting industry. Overall, the focus of carbon emission reduction in metal smelting should be placed on energy structure adjustment, and active industrial low-carbon transformation is a critical way to achieve carbon emission reduction.

Figure3:Ridge trace map

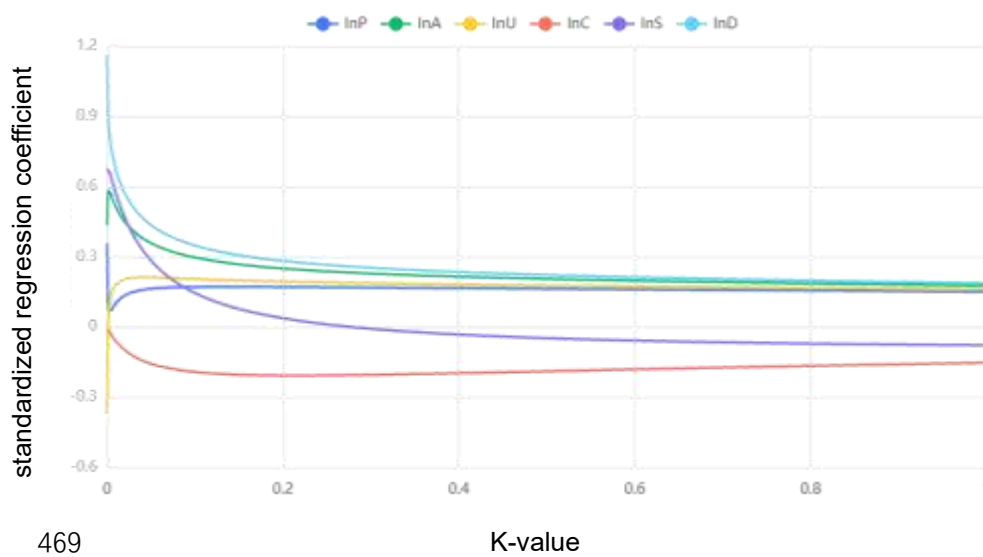


Table 6:Results of Ridge Regression Analysis

K=0.034	Non-normalized		Standardized		t	P	R²	AdjustedR²	F
	coefficients		coefficient						
	Standard		Beta						
	B	Error							
Constants	-	5.175	-	-1.265	0.228				
	6.548								
lnP	2.078	0.691	0.154	3.005	0.010**	0.987	0.981	163.837(0.000***)	
lnA	0.251	0.023	0.396	11.127	0.000***				
lnU	0.564	0.09	0.211	6.277	0.000***				

InC	-	0.368	-0.133	-3.636	0.003***
	1.339				
InS	0.485	0.098	0.365	4.928	0.000***
InD	0.318	0.032	0.492	9.797	0.000***
Dependent variable: InI					

Note : * * *, * *, * represents the significance level of 1 %, 5 %, 10 % respectively

471 **4 Metal smelting carbon emission scenario setting**

472 (1) Population. From the historical data between 2001 and 2020, China's population
473 growth has shown a significant slowdown, and even since the implementation of the
474 open two-child policy in 2016, the average annual growth rate in the five years is only
475 0.28%, while China's annual births have been declining for four consecutive years since
476 2017. on May 31, 2021, the three-child birth policy will be implemented, stimulating
477 China's population growth to some extent. Based on the experience of the fertility
478 potential brought about by the "full two-child" policy, it is expected that the fertility
479 potential brought about by this policy will be released within 3-5 years. According to
480 the China Population and Development Research Center, China's population will peak
481 at 1.417 billion in 2027. It will continue to grow negatively after that, dropping to 1.403
482 billion in 2035 and 1.321 billion in 2050.

483 (2) GDP. China's GDP growth rate dropped to 2.3% in 2020 due to the severe impact
484 of the new pneumonia epidemic, with a year-on-year growth rate of 4%. Since 2021,
485 the economy has gradually recovered, with market-related institutions forecasting a
486 GDP growth rate of around 8%. China's 14th Five-Year Plan and the proposed 2035
487 Vision also clearly set the goal of doubling the total economic volume or per capita
488 income by 2035. Accordingly, the annual change rate of GDP is set between 8% and
489 10% in this paper.

490 (3) Urbanization rate. The urbanization rate of China's population reached 63.89% in
491 2020, while the urbanization rate of developed countries in the world exceeds 80% and

tends to be stable. "During the 14th Five-Year Plan period, China's urbanization rate is expected to increase by 1.03% annually, which is lower than that of the 13th Five-Year Plan period. According to the Green Paper on Population and Labor published by the Institute of Population and Labor Economics, Chinese Academy of Social Sciences, the growth rate of China's urbanization will slow down during the 14th Five-Year Plan period. It will show a relatively stable trend after 2035, with a peak rate of 75% to 80%.

(4) Energy structure. The white paper "China's Green Development in the New Era" points out that China has, based on its energy resource endowment, insisted on establishing before breaking, planned holistically, accelerated the construction of a new energy system based on continuously enhancing the energy supply guarantee capacity, promoted a significant increase in the proportion of clean energy consumption, and achieved remarkable results in a green and low-carbon transformation of energy structure. In recent years, China's coal consumption has declined as a proportion of total energy consumption. By the end of 2021, clean energy consumption rose from 14.5% in 2012 to 25.5%, and coal consumption fell from 68.5% in 2012 to 56.0%, down 0.9% from the previous year. The trend is to reduce the proportion of coal consumption, which is the only way to achieve a "carbon peak, carbon neutral."

(5) Energy consumption intensity. The Blue Book on China's Low Carbon Economy Development Report (2022-2023) (from now on referred to as the "Blue Book on Low Carbon Economy") shows that in 2022, national energy consumption per 10,000 yuan of gross domestic product (GDP) will decrease by 0.1%. Carbon dioxide emissions per 10,000 yuan of GDP will decrease by 0.8% compared with the previous year, and energy conservation, consumption reduction, and emission reduction will be steadily promoted. Since 2012, China has been able to Since 2012, China has supported an average annual economic growth of 6.6% with an average annual growth rate of 3% in energy consumption, and energy consumption per unit of GDP has dropped by 26.4%, making it one of the countries with the fastest reduction in energy consumption intensity

in the world. The Blue Book on Low Carbon Economy points out that for a long time, China's carbon dioxide emissions have kept pace with economic growth, indicating that China's economic growth is still mainly driven by crude resource consumption and has yet to be decoupled from carbon emissions. In the decade of the new era, China's low-carbon economic development has made world-renowned achievements, with a cumulative decrease of 26.2% in energy consumption intensity, equivalent to using 1.4 billion tons of standard coal less and emitting 2.94 billion tons of carbon dioxide less, and the decrease in carbon dioxide emission intensity per unit of GDP exceeding the goal of independent contribution. In 2022, China's energy consumption per unit of GDP will drop by 13.5% compared to 2020. unit In 2022, China's energy consumption per unit of GDP will drop by 13.5% compared with 2020. CO2 emissions per unit of GDP will drop by 18% compared with 2020. a solid foundation has been laid for achieving carbon peaking and carbon neutrality.

(6) Value added of the secondary industry. The secondary industry is the pillar industry in the development of the national economy, and its development level is an important symbol to measure the degree of socialization of production and the level of development of the market economy. The Statistical Bulletin on National Economic and Social Development of the People's Republic of China for 2022 pointed out that China's annual gross domestic product in 2022 was RMB 1,120,207 billion, an increase of 3.0% over the previous year. The added value of the primary industry was 8,834.5 billion yuan, up 4.1% over the previous year, the added value of the secondary industry was 4,831.64 billion yuan, up 3.8%, and the added value of the tertiary industry was 6,386.98 billion yuan, up 2.3%. The ratio of the secondary industry's added value to GDP from 2018 to 2022 was 39.7%, 38.6%, 37.8%, 39.3%, and 39.9%, respectively. In this paper, regarding the relevant policies and plans promulgated by the state, the scenario model is set as low-carbon, standard, and high-carbon models, and the rate of

change of each factor is set according to the overall trend and annual average rate of change of each factor in recent years.

Table 7:China Metal Smelting Carbon Emissions Scenario Setting

Annual change rate (%)					
Contextual model	PGDP	Urbanization rate	Energy structure	Energy consumption intensity	The added value of the secondary industry
Low-carbon	8	0.5	-0.5	-0.085	3.8
Standard	9	0.7	-0.45	-0.08	4
High-carbon	10	0.9	-0.4	-0.075	4.2

Due to the particular future growth trend of China's population, the annual rate of population change is set in this paper as follows:

Table 8: Annual rate of population change setting

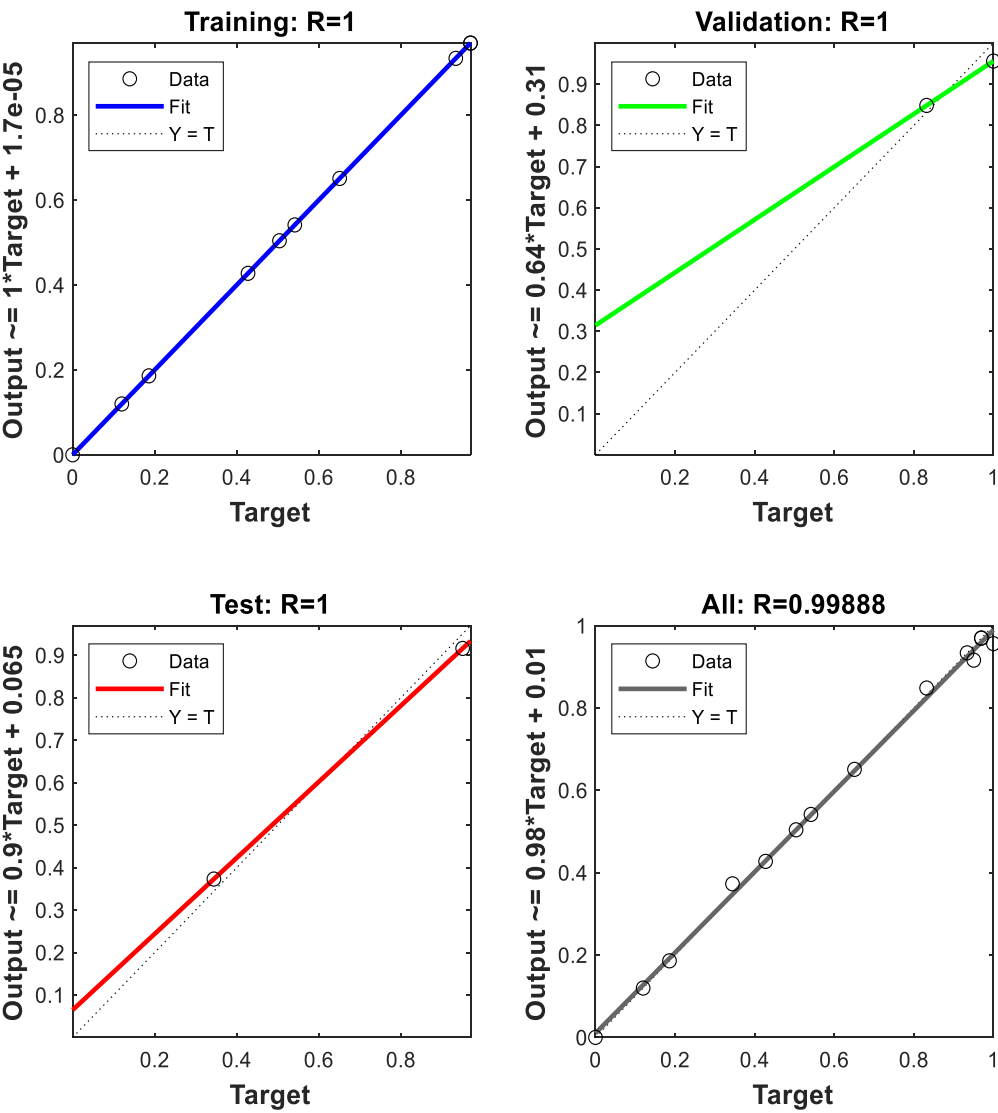
Annual change rate (%)			
Year	Low-carbon	Standard	High-carbon
2021-2027	0.04	0.05	0.06
2028-2035	-0.15	-0.1	-0.05
2036-2050	-0.45	-0.4	-0.35

5 Validation and prediction of PSO-BP model for carbon emissions from metal smelting

5.1 PSO-BP model validation

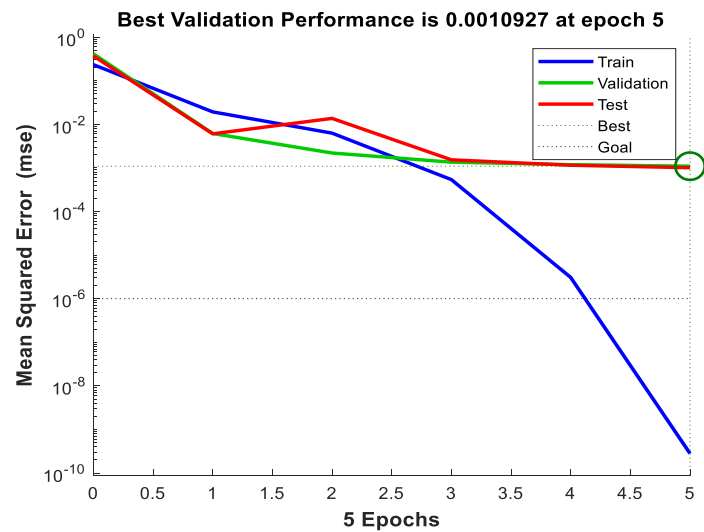
After the basic parameters of the particle swarm algorithm and neural network are set, the PSO-BP model is continuously trained using MATLAB software to optimize the parameters and logical structure to ensure that the training results can fully reflect the actual situation of carbon emissions from metal smelting in China.

Figure 4: Performance of PSO-BP model

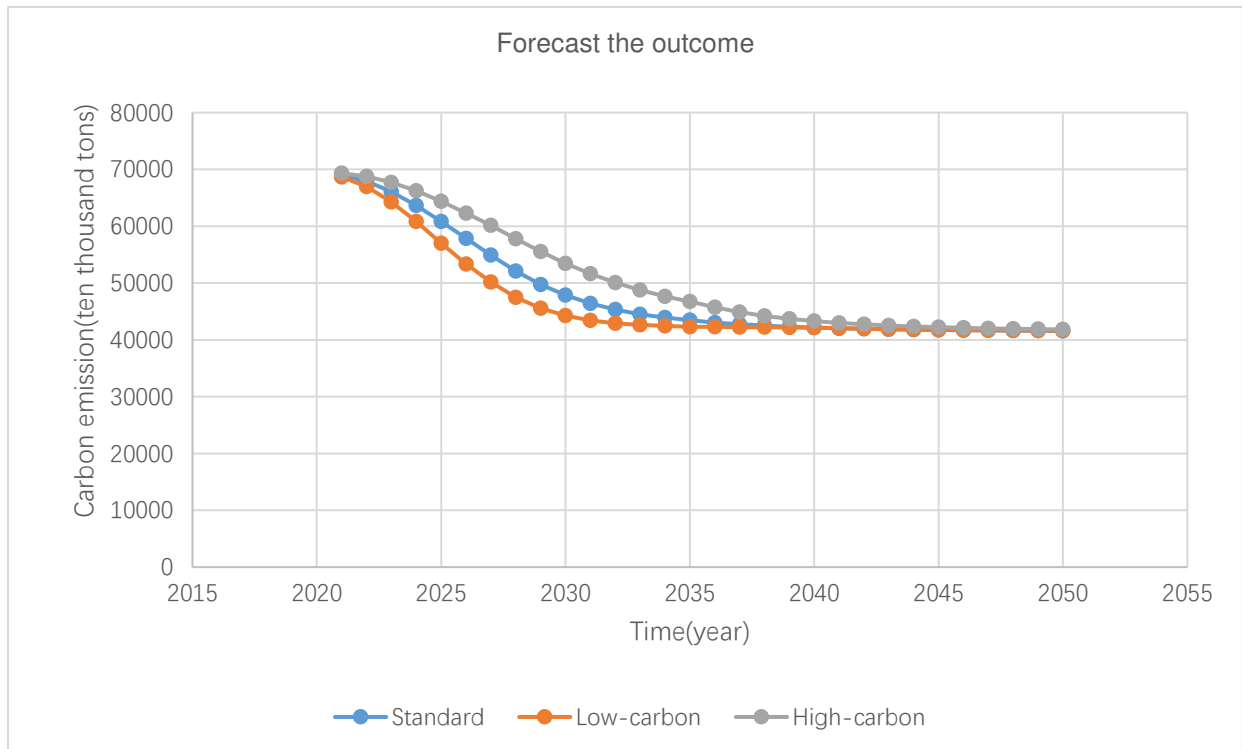


559 As can be seen from Figures 4 and 5, the trained PSO-BP model has good performance
560 and is suitable for prediction. In addition, the mean square error of the trained model is
561 0.0027638, which is a small error, indicating that the model can predict the carbon
562 emissions of China's metal smelting industry more accurately.

Figure 5: Performance analysis of PSO-BP model in training, testing and validation phases



5.2. Scenario Projection Results



The decreasing trend of China's metal smelting carbon emissions in 2021-2050 indicates that China's metal smelting carbon emission reduction efforts are practical and feasible. According to the data of previous years and the forecast results, under the baseline model, low-carbon model, and high-carbon model, China's metal smelting

carbon emissions reached the historical peak of 727,963,200 tons in 2014, and the carbon emissions under all three models developed in a decreasing trend year by year, indicating that China's metal smelting carbon emission reduction potential is still considerable.

6 Conclusion

In this paper, the STIRPAT model was used to analyze the factors influencing the carbon emissions of metal smelting in China, and the PSO-BP neural network model was used to forecast the carbon emissions of metal smelting in China from 2020 to 2050. The main research results are as follows.

(1) In terms of the overall carbon emission trend, the total carbon emission of metal smelting in China from 2001 to 2020 is 10,581,991,400 tons, and it developed in a decreasing trend year by year after reaching the peak in 2014. This indicates that China's metal smelting has achieved a 'carbon peak' and laid a good foundation for achieving 'carbon neutral.'

(2) From the analysis of carbon emission influencing factors, population, GDP, urbanization rate, energy consumption intensity, and value-added of the secondary industry have a catalytic effect on carbon emission in China's metal smelting industry. Energy structure has a suppressive effect on China's metal smelting industry. It indicates that there is still much room for progress in implementing carbon emission reduction in China's metal smelting industry.

(3) In terms of sensitivity, the sensitivity of each factor is ranked from highest to lowest: population size, energy structure, urbanization rate, energy consumption intensity, value added of secondary industry, and GDP per capita. The population has the most significant effect on carbon emissions, indicating that population size indirectly increases energy consumption and carbon emissions. Energy structure has the most significant inhibiting effect on carbon emissions, indicating that accelerating energy

structure adjustment is a powerful means to promote carbon emission reduction in metal smelting.

(4) In terms of the prediction model, the PSO-BP model has a small error and good prediction performance, and the prediction results can fully reflect the actual situation of carbon emissions from metal smelting in China. Thus the accuracy of the BP neural network model was significantly improved under the optimization of the particle swarm (PSO) algorithm, and the accuracy of the PSO-BP model for carbon emission prediction was verified in this study, which is in line with most of the current research findings.

7 Policy Suggestions

In order to promote the metal smelting industry to transform its energy structure, encourage metal smelting enterprises to develop non-fossil energy, and help China successfully achieve the goal of carbon neutrality, this paper puts forward the following policy recommendations.

(1) Improve the carbon trading market and system to improve the enthusiasm of enterprises to reduce carbon emissions. Through the market mechanism to enhance the metal smelting industry's awareness of low carbon development, the use of carbon emission costs to force metal smelting enterprises to use non-fossil energy to replace fossil fuels and promote the transformation of the production energy structure of the metal smelting industry.

(2) Strengthen top-level design and strategic guidance. According to the actual situation of the region, the overall planning of non-fossil energy use gives full play to the advantages of the region's natural conditions. It encourages metal smelting enterprises to develop non-fossil energy following local conditions.

(3) Guide metal smelting enterprises to develop non-fossil energy through policy guidance and financial support. For example, the use of wind, light, water power, biomass, and other energy generation can obtain additional hours of power generation through the green credit business to obtain more financing for the use of non-fossil

energy to promote the transformation and upgrading of the energy structure of the metal smelting industry.

(4) Increase the exchange and cooperation between the metal smelting and non-fossil energy industries. Establish an exchange platform between the metal smelting industry and the non-fossil energy industry, promote the sharing of information and consultation between the industries, raise the awareness of the metal smelting industry on the application of non-fossil energy resources, and promote the energy structure upgrade and high-quality development of the traditional metal smelting industry.

(5) Promote the digital upgrade of the energy control platform of the metal smelting industry. Promote the application and upgrade of information-based and intelligent energy control systems, enhance the control and scheduling of multi-energy systems in metal smelting enterprises, and improve the construction and optimization of energy flow networks in the industry.

Author contributions

Xinfa Tang: conceptualization and writing—review and editing, and supervision. Lui Shuai: conceptualization, methodology, writing—original draft preparation, writing—review, and editing, and resources. Wang Yonghua: conceptualization, methodology, formal analysis, investigation, writing—original draft preparation, and writing—review and editing. Wan Youwei: methodology, writing—original draft preparation, resources, and resources..

Data availability statement

The original contributions presented in the study are included in the article/Supplementary Materials, further inquiries can be directed to the corresponding author.

Declarations

Ethical approval Not applicable.

Consent to participate All the participants in this study were recruited with available informed consent.

Consent for publication All authors are informed and agree to the study.

Competing interests The authors declare no competing interests.

Funding

This work was financially supported by the Science and Technology Research Project of Jiangxi Education Department (Project number: GJJ2201327) .

References

Adebayo, T.S., Oladipupo, S.D., Rjoub, H. et al. Asymmetric effect of structural change and renewable energy consumption on carbon emissions: designing an SDG framework for Turkey. *Environ Dev Sustain* 25, 528–556 (2023). <https://doi.org/10.1007/s10668-021-02065-w>

Ali, H.S., Sahoo, M., Alam, M.M. et al. Structural transformations and conventional energy-based power utilization on carbon emissions: empirical evidence from Pakistan. *Environ Dev Sustain* 25, 2419–2442 (2023). <https://doi.org/10.1007/s10668-022-02133-9>

Cai Jingli, Gu Jiayan, Chen Min, Xie Liping, He Guofu. Analysis of carbon emission drivers and projections of China's plantation industry from 2000 to 2020[J].*Environmental Science and Technology*,2023,46(02):159-167.DOI:10.19672/j.cnki.1003-6504.1841.22.338.

Huang, Y., Liu, J. & Shi, M. Analysis of influencing factors and prediction of carbon emissions of typical urban agglomerations in China: a case study of Beijing-Tianjin-Hebei region. *Environ Sci Pollut Res* 30, 52658–52678 (2023). <https://doi.org/10.1007/s11356-023-26036-y>

Islam, M.S., Rahaman, S.H. The asymmetric effect of ICT on CO2 emissions in the context of an EKC framework in GCC countries: the role of energy consumption, energy intensity, trade, and financial development. *Environ Sci Pollut Res* (2023). <https://doi.org/10.1007/s11356-023-27590-1>

Li Yuanqi, Zhou Lei, Gao Peiqi, Yang Bo, Han Yiming, Lian Chang. Short-Term Power Generation Forecasting of a Photovoltaic Plant Based on PSO-BP and GA-BP Neural Networks[J]. *Frontiers in Energy Research*, 2022.

Li, Y., Li, T. & Lu, S. Forecast of urban traffic carbon emission and analysis of influencing factors. *Energy Efficiency* 14, 84 (2021). <https://doi.org/10.1007/s12053-021-10001-0>

681 Lin X, Lin X, Zhang J, He Q, Yan P. Simulation Analysis of Factors Affecting Energy
682 Carbon Emissions in Fujian Province. Sustainability. 2022. 14(21):13757.
683 <https://doi.org/10.3390/su142113757>

684 Liping Zhu. Zhizhong Li. Xubiao Yang. Yili Zhang. Hui Li. Forecast of Transportation
685 CO2 Emissions in Shanghai under Multiple Scenarios[J]. Sustainability, 2022, Vol.
686 14(13650): 13650

687 Liu YK, Jin STS. Spatial and temporal evolution characteristics and influencing factors
688 of carbon emissions from energy consumption in six central provinces[J]. Economic
689 Geography,2019,39(01):182-191.DOI:10.15957/j.cnki.jjdl.2019.01.022.

690 Lv, T., Hu, H., Xie, H. et al. An empirical relationship between urbanization and carbon
691 emissions in an ecological civilization demonstration area of China based on the
692 STIRPAT model. Environ Dev Sustain 25, 2465–2486 (2023).
693 <https://doi.org/10.1007/s10668-022-02144-6>

694 Ma Xiaojun, Chen Ruimin, Su Heng. Analysis of the drivers and decoupling of energy
695 consumption in Chinese industrial sectors[J]. Statistics and Information
696 Forum,2021,36(03):70-81.

697 Mutascu, M. CO2 emissions in the USA: new insights based on ANN approach.
698 Environ Sci Pollut Res 29, 68332–68356 (2022). [https://doi.org/10.1007/s11356-022-](https://doi.org/10.1007/s11356-022-20615-1)
699 20615-1

700 Nie, W., Ao, O. & Duan, H. A novel grey prediction model with a feedforward neural
701 network based on a carbon emission dynamic evolution system and its application.
702 Environ Sci Pollut Res 30, 20704–20720 (2023). [https://doi.org/10.1007/s11356-022-](https://doi.org/10.1007/s11356-022-23541-4)
703 23541-4

704 Pan Chongchao, Wang Bowen, Hou Xiaowang, Gu Yueqing, Xing. YI, Liu Yusong,
705 Wen Wei, Fang Juan. Study on the carbon peaking path in Chinese iron and steel
706 industry based on LMDI-STIRPAT model[J]. Journal of Engineering
707 Science,2023,45(06):1034-1044.DOI:10.13374/j.issn2095-9389.2022.04.25.002.

708 Pu X, Yao J, Zheng R. Forecast of Energy Consumption and Carbon Emissions in
709 China's Building Sector to 2060. Energies. 2022. 15(14):4950.
710 <https://doi.org/10.3390/en15144950>

711 Qader, M.R., Khan, S., Kamal, M. et al. Forecasting carbon emissions due to electricity
712 power generation in Bahrain. *Environ Sci Pollut Res* 29, 17346–17357 (2022).
713 <https://doi.org/10.1007/s11356-021-16960-2>

714 Qiaochu Li, Junhua Chen, Jing He. Prediction of regional carbon emission trends in the
715 medium and long term based on system dynamics-Visual Studio integrated model--
716 Sichuan Province as an example[J]. *Environmental Pollution and Prevention*,
717 2022,44(12):1669-1675.DOI:10.15985/j.cnki.1001-3865.2022.12.021.

718 Qin, X., Zhang, S., Dong, X., et al. China's carbon dioxide emission forecast based on
719 improved marine predator algorithm and multi-kernel support vector regression.
720 *Environ Sci Pollut Res* 30, 5730–5748 (2023). [https://doi.org/10.1007/s11356-022-](https://doi.org/10.1007/s11356-022-22302-7)
721 [22302-7](https://doi.org/10.1007/s11356-022-22302-7)

722 Shi, M. Forecast of China's carbon emissions under the background of carbon neutrality.
723 *Environ Sci Pollut Res* 29, 43019–43033 (2022). [https://doi.org/10.1007/s11356-021-](https://doi.org/10.1007/s11356-021-18162-2)
724 [18162-2](https://doi.org/10.1007/s11356-021-18162-2)

725 Sun, J., Guo, X., Wang, Y. et al. Nexus among energy consumption structure, energy
726 intensity, population density, urbanization, and carbon intensity: a heterogeneous panel
727 evidence considering differences in electrification rates. *Environ Sci Pollut Res* 29,
728 19224–19243 (2022). <https://doi.org/10.1007/s11356-021-17165-3>

729 Tang X.L., Liu J.M. Prediction of peak building carbon emissions based on PSO-LSTM
730 network model[J]. *Science and Technology Management Research*,2023,43(01):191-
731 198.

732 Tong, M., Duan, H. & He, L. A novel Grey Verhulst model and its application in
733 forecasting CO₂ emissions. *Environ Sci Pollut Res* 28, 31370–31379 (2021).
734 <https://doi.org/10.1007/s11356-020-12137-5>

735 Verbič, M., Satrovic, E. & Mujtaba, A. Assessing the Driving Factors of Carbon
736 Dioxide and Total Greenhouse Gas Emissions to Maintain Environmental
737 Sustainability in Southeastern Europe. *Int J Environ Res* 16, 105 (2022).
738 <https://doi.org/10.1007/s41742-022-00486-7>

739 Wang H, Li B, Khan MQ. Prediction of Shanghai Electric Power Carbon Emissions
740 Based on Improved STIRPAT Model. *Sustainability*. 2022. 14(20):13068.
741 <https://doi.org/10.3390/su142013068>

742 Wang, M., Wu, L. & Guo, X. Application of grey model in influencing factors analysis
743 and trend prediction of carbon emission in Shanxi Province. *Environ Monit Assess* 194,
744 542 (2022). <https://doi.org/10.1007/s10661-022-10088-7>

745 Xiao H, Deng ZH, Ren YJ, Ren XH. Carbon emission prediction model and carbon
746 reduction strategy for urban transportation [J/OL]. *Journal of Chongqing Jiaotong*
747 *University (Natural Science Edition)*:1-10 [2023-04-23].

748 Yan Li. Forecasting Chinese carbon emissions based on a novel time series prediction
749 method[J]. *Energy Science & Engineering*,2020,8(7).

750 Zhang J, Liu JY, Dong L, et al. Influencing factors and scenario analysis of CO2
751 emissions from energy consumption in China[J]. *Journal of Environmental Engineering*
752 *Technology*,2023,13(01):71-78.

753 Zhang Qingyu, Zhang Yulong, Pan Binbin. Analysis of factors influencing economic
754 growth and carbon emissions in China in the 40 years of reform and opening up[J]. *Arid*
755 *Zone Resources and Environment*,2019,33(10):9-13.DOI:10.13448/j.cnki.jalre.
756 2019.280.

757 Zhang Zhe, Ren Yimeng, Dong Huijuan. Research on urban carbon emission peaking
758 and low carbon development: A case study of Shanghai[J]. *Environmental*
759 *Engineering*,2020,38(11):12-18.DOI:10.13205/j.hjgc.202011003.

760 Zhang, C.. Zou, X.. Lin, C. Carbon Footprint Prediction of Thermal Power Industry
761 under the Dual-Carbon Target: A Case Study of Zhejiang Province,
762 China. *Sustainability* 2023, 15, 3280. <https://doi.org/10.3390/su15043280>

763 Zhao C, Song X. C., Liu X. Y., Shen P., Chen C., Liu L. Analysis of carbon emission
764 peak prediction in Zhejiang Province based on STIRPAT model[J]. *Ecological*
765 *Economics*,2022,38(06):29-34.

766 Zou Xiuqing, Sun Xuecheng, Ge Tianyue, Xing Sheng. Differences in carbon emissions
767 in the Yangtze River Delta region, their impact mechanisms and carbon peak
768 projections[J]. *Yangtze River Basin Resources and Environment*,2023,32(03):548-557.